FULL PAPER

Proton Motion and Proton Transfer in the Formamidine–Formic Acid Complex: An Ab Initio Projector Augmented Wave Molecular Dynamics Study

Alexandra Simperler,[a, b] Werner Mikenda,*[a] and Karlheinz Schwarz[c]

Abstract: An ab initio molecular dynamics study performed with the projector augmented wave method (PAW) on proton motion and (double) proton transfer in the formamidine–formic acid complex is reported. The PAW trajectories were calculated with a time interval of 0.12 fs, for a total evolution time period of 36 ps, and for temperatures in the range 500–600 K. All proton-transfer processes start with a proton transition at the $O-H \cdots N$ group, and are followed by a second proton transition, either at the same group ("single crossing–recrossing transitions") or at the other group, namely the $N-H \cdots O$ group ("double proton transfers"). According to the delay between the two transitions (more or less than 15 fs), one may distinguish between "concerted" (42%) or "successive" (16%) single crossing–recrossing transitions, and between "simultaneous" (7%) or "successive" (35%) double proton transfers. Successive processes take place via a zwitterionic intermediate, which remains stable for up to approximately 120 fs ("ionic regions"). The findings are in excellent agreement with the results of ab initio (HF, MP2) and density functional theory (DFT; B3LYP, B3P86) calculations, according to which the zwitterionic intermediate that results from the first proton transition is a true local minimum. Furthermore, it is shown that the optimized geometries of stationary points (ground state, transition state, and zwitterion) comply well with corresponding average data obtained from the PAW trajectories for normal periods, crossover points, and ionic regions.

Introduction

We previously reported projector augmented wave (PAW)[1] molecular dynamics studies about proton motion and proton transfer in some selected strongly hydrogen-bonded compounds that are capable of proton transfer: malonaldehyde,[2] which is the most prominent model system for intramolecular proton transfer, 5,8-dihydroxy-1,4-naphthoquinone (DHN),[3] which provides an example of an intramolecular double proton transfer, and the formic acid dimer (FAD),[3] which is the most simple model system for intermolecular double proton transfer. It was shown that in the case of DHN, double proton transfer takes place preferably by a consecutive two-step mechanism (i.e., two successive proton transitions), whereas in the case of FAD, double proton transfer takes place almost exclusively by a concerted mechanism that almost simultaneously involves both $O-H \cdots O$ groups. In both cases, the findings complied excellently with the results of ab initio and density functional theory (DFT) calculations on transition states and metastable intermediates. The method employed in these studies, PAW, is a variant of the ab initio molecular dynamics approach of R. Car and M. Parrinello[4] (see ref. [5] for recent CPMD studies). PAW is the first all-electron method and owing to its sophisticated augmentation scheme, is computationally highly feasible. PAW allows for finite-temperature molecular dynamics simulations for relatively long time periods (i.e., on a picosecond time scale) and/or for relatively large systems within reasonable cpu time (see ref. [6] for some recent PAW studies). Since all nuclear motions are treated classically, PAW does not account for quantum effects such as proton tunneling or zero-point motion. Hence the PAW simulations establish a high-temperature approach for dynamic processes, where quantum phenomena are negligible to a first approximation.

[a] Prof. Dr. W. Mikenda, Dr. A. Simperler
Institut für Organische Chemie
Universität Wien, Währingerstrasse 38
1090 Vienna (Austria)
Fax: (+431) 4277 9521
E-mail: Werner.Mikenda@univie.ac.at

[b] Dr. A. Simperler
Present address:
The Royal Institution of Great Britain, 21 Albemarle Street
London W1S 4BS (UK)

[c] Prof. Dr. K. Schwarz
Institut für Physikalische Chemie und Theoretische Chemie
Technische Universität Wien, Getreidemarkt 9, 1060, Vienna (Austria)

Herein, we supplement these PAW proton-transfer studies with another example, the formamidine – formic acid complex (FFA). Along with the guanidine – formic acid complex, FFA is a popular model system for the theoretical investigations of biologically relevant hydrogen-bonded complexes that involve one O−H···N and one N−H···O bond.[7, 8] For example, carboxylic groups of glutamic or aspartic acid are well known to form highly specific complexes with the guanidinium moiety of arginine. These complexes play an important role in protein recognition, stabilization, or enzyme – substrate interactions (i.e., carboxylic substrate fixation).[9] According to the most recent ab initio and DFT calculations,[8] the most stable configuration of FFA in the vapor phase is the neutral, doubly hydrogen-bonded complex (structures **1** and **2** in Figure 1).
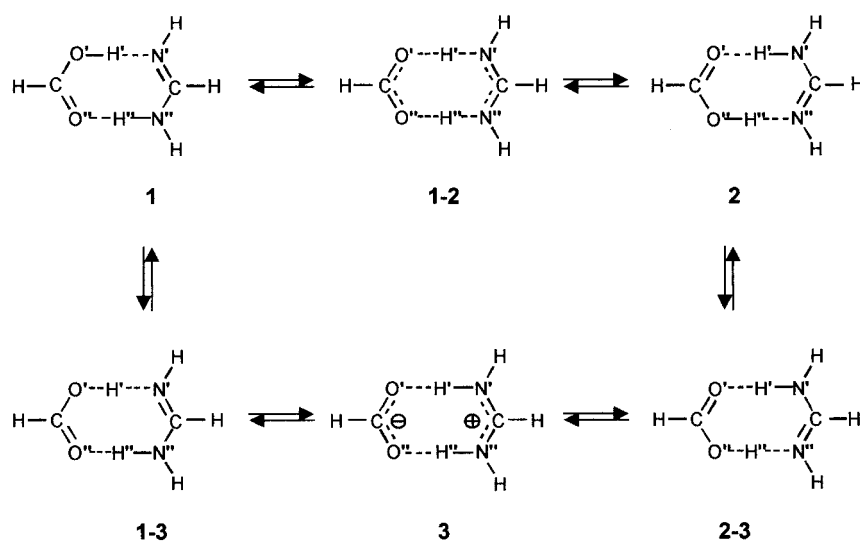

Figure 1. Prototropic isomers and proton transfer transition states of the formic acid – formamidine complex (FFA).

For the barrier height, that is the energy difference between **1** and **1-3** (or between **2** and **2-3**), values between 8.27 (at the HF/6-31G(d,p) level) and 1.64 kcal mol^{-1} (at the B3LYP/6-31G+(d,p) level) were obtained; 3.95 kcal mol^{-1} resulted from the highest level CCSD(T)//MP2/6-31G+(d,p) calculation. Furthermore, at all computational levels, the formamidinium – formate ion pair **3** was found to be a relatively shallow local minimum approximately 0.3 kcal mol^{-1} below the transition states. Based on their results, the authors claimed that double proton transfer in FFA occurs asynchronously via the metastable zwitterionic intermediate **3**.

In the following, we present time evolutions of R(OH) and R(HN) bond lengths to visualize the most prominent features of the molecular-dynamics simulations of FFA. Based on various blow-ups of these time evolutions, we qualitatively discuss typical situations within the "active" periods in which proton transitions and proton-transfer processes take place. We inspect the average hydrogen-bond geometries and the respective changes associated with typical situations, and we compare these data with those obtained from geometry optimizations (ab initio and DFT) of the prototropic species shown in Figure 1. We also show that theoretical energy data comply excellently with the results of the molecular-dynamics simulations. Finally, we discuss similarities and differences

between the preferred double proton-transfer mechanisms in FFA, DHN, and FAD.

Methods

The PAW molecular dynamics simulations were performed with constant time intervals of 0.1209 fs (= 5 au) for a total evolution time period of 36 ps (about 300 000 single time steps). The temperatures of the molecular dynamics runs (between 500 K and 600 K) were controlled with the Nosè – Hoover thermostat[10] with a frequency of 15 THz for the Nosè variable. At the beginning of a run, random velocities were added; the velocity distributions corresponded to temperatures of 150 to 200 K above the subsequent constant-simulation temperature. Perdew and Zunger's parametrization of the density functional[11] (based on the results of Ceperley and Alder,[12]) was used, and the generalized gradient correction of Becke and Perdew was applied.[13] The cut-off of the plane wave part of the basis functions was 30 Ry (= 15 au), whereas for the charge density, a cut-off of 60 Ry (= 30 au) was chosen. The plane waves were augmented with s-type projector functions for hydrogen atoms, and with s-type and p-type projectors for carbon, nitrogen, and oxygen atoms.

Supplementary to PAW simulations, optimized geometries and vibrational frequencies were calculated for the prototropic species of Figure 1 with the Gaussian98 programs[14] at several levels of theory (HF, MP2, B3LYP, and B3P86) using the 6-31G++(d,p) basis set. As previously noted,[3] energy and geometry data obtained with the B3P86 functional are, on average, closest to the corresponding zero-temperature PAW data. The structures were fully optimized at all levels of theory, and each stationary point was characterized by harmonic-frequency analysis.

Results and Discussion

PAW trajectories:[15] Figure 2 displays time evolutions of the R(OH) and R(NH) distances of the two hydrogen atoms, H′ and H″, for a time period of 6 ps (i.e. a total of approximately 50 000 single time steps) at a temperature of 500 K. At that temperature, the number of processes observed within reasonable cpu time was large enough for the intended statistical evaluation. As in our previous studies, two fundamental situations can be clearly distinguished: 1) "normal periods", in which R(OH′) and R(NH′) trajectories, as well as R(OH″) and R(NH″) trajectories, remain clearly separated from each other (see also Figure 3a). In this case, the two hydrogen atoms remain trapped at one of the two bridging atoms (oxygen or nitrogen) and undergo (quasi)stationary motions with average amplitudes of approximately 10 pm; and 2) "active periods", which are characterized by crossover points of corresponding R(OH) and R(NH) trajectories of one or both hydrogen atoms (see also Figures 3b–f). In this case, one or both hydrogen atoms undergo nonstationary, large-amplitude motions (typically 30 pm), by which they move from one to the other bridging atom.
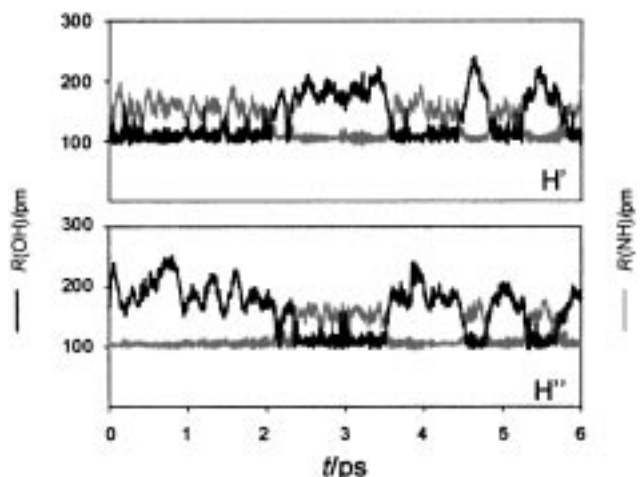
Figure 2. Time evolution of the R(OH) (black traces) and R(HN) (gray traces) distances for H′ (initial O−H···N group) and H″ (initial N−H···O group).

Some typical situations and processes are illustrated in more detail in Figure 3 by blow-ups (time periods of 120 fs) of the R(OH) and R(NH) time evolutions of the two hydrogen atoms, H′ and H″. In the normal period shown in Figure 3a, the above-mentioned stationary proton motions that correspond to common ν(OH) and ν(NH) stretching vibrations are clearly evident; the average frequencies are 70 THz (2400 cm^{-1}) and 100 THz (3300 cm^{-1}), respectively.

Within the active periods, 58% of the observed events are "single" proton-transfer processes, where activity is confined to the initial O−H···N group, while the initial N−H···O group is not involved. Similar to previous studies,[2, 3] these single processes may be classified as: 1) "concerted crossing–recrossing transitions" (32%), in which the proton moves from the oxygen atom to the nitrogen atom, and then almost immediately, with a delay of less than 15 fs as measured by the difference between the two crossover points, moves back to the oxygen atom: O−H···N → O···H−N → O−H···N (Figure 3b); 2) "proton-shuttling periods" (10%), in which the proton undergoes several consecutive concerted crossing–recrossing transitions: O−H···N → O···H−N → O−H··· N → O···H−N → O−H···N →→ (Figure 3c); and 3) "successive crossing–recrossing transitions" (16%), in which the proton moves from the oxygen atom to the nitrogen atom, and after a delay of more than 15 fs (the maximum delay observed was 115 fs), moves back to the oxygen atom: O−H···N → O···H−N → O−H···N (Figure 3d).

A large part of the events within the active periods (42%) are "double" proton-transfer processes, where activity at the initial O−H···N group is followed by activity at the initial N−H···O group: O−H···N → O···H−N followed by N−H···O → N···H−O. Analogously to the above distinction between "concerted" and "successive" crossing–recrossing transitions, the double proton-transfer processes may be classified according to the delay between the two proton transitions as
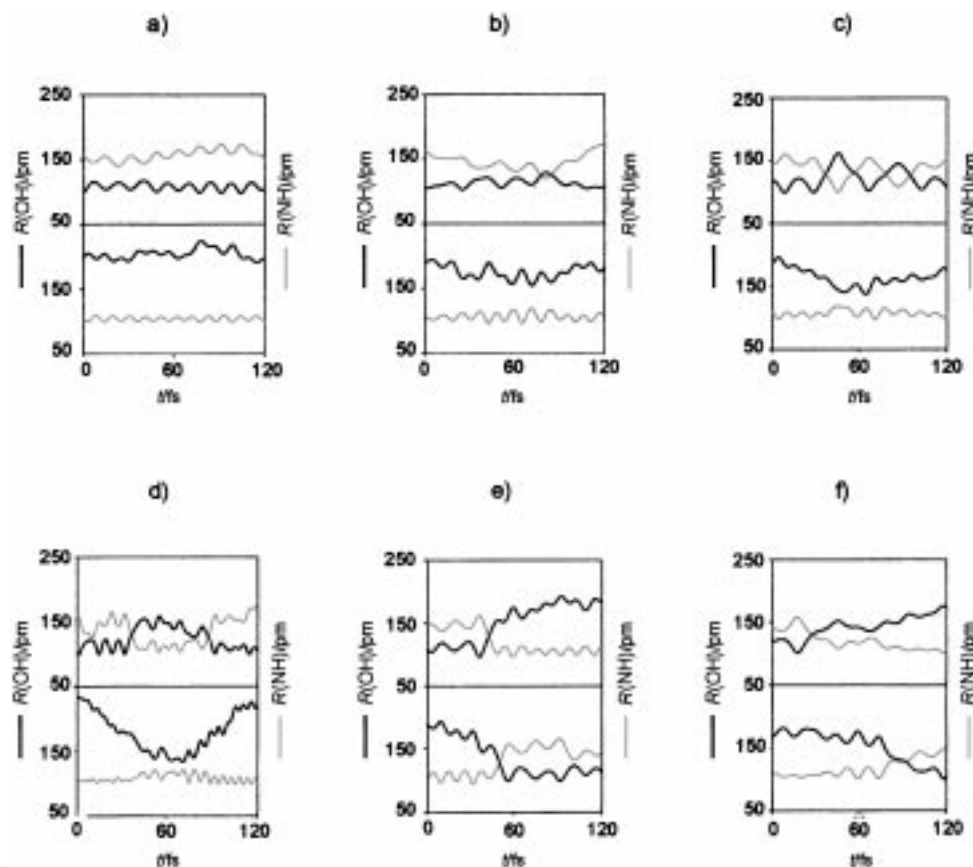

Figure 3. Time evolution of the R(OH) (black traces) and R(HN) (gray traces) distances, showing: a) a normal period, b) a concerted crossing–recrossing transition, c) a single proton shuttling period, d) a successive crossing–recrossing transition, e) a simultaneous double proton-transfer process, f) a successive double proton-transfer process.

"simultaneous processes" (7 %), with a delay of less than 15 fs (the minimum delay observed was 7 fs) (Figure 3e), or "successive processes" (35 %) with a delay of more than 15 fs (the maximum delay observed was 120 fs) (Figure 3f).

Although the limiting delay of 15 fs that was chosen to distinguish between the different processes may be somewhat arbitrary, it does have a distinct physical meaning. Essentially, an O−H···N → O···H−N proton transition, which is the first step for all the processes, should result in a zwitterionic intermediate and the classification raises the question of whether or not such a metastable intermediate is actually formed during a process. A delay of 15 fs between the crossover points of the O−H···N → O···H−N and the following N−H···O → N···H−O transition means that the zwitterion exists for a time period that corresponds to an average $\nu(NH)$ vibrational cycle, which seems to be a reasonable criterion for a definite formation or existence of an intermediate. Likewise, we can also define a "true proton transfer", if the proton becomes trapped at the nitrogen atom for at least 15 fs. Accordingly, with all successive single and double processes, a zwitterionic intermediate is formed by a true proton transfer at the initial O−H···N group, which after some delay (between 15 and 120 fs) becomes restabilized by a second true proton transfer that may involve either the same or the other proton, H′ (= crossing–recrossing) or H″ (= double proton transition) (Figures 3d, f). Simultaneous double proton-transfer processes also start with a true proton transfer at the initial O−H···N group, but the proton transfer at the initial N−H···O group follows almost immediately, so that the zwitterionic intermediate is not definitely formed (Figure 3e). On the other hand, concerted crossing–recrossing transitions and shuttling periods do not involve true proton transfers. Instead, crossing and recrossing are branches of a smooth, large-amplitude proton motion between the two bridging atoms, that is, parts of an outstanding nonstationary large-amplitude vibration,[2, 3] without the definite formation of an intermediate (Figures 3b, c).

Hydrogen bond lengths: For a more detailed analysis of the geometric features observed within the PAW trajectories, a sample data set was constructed that contained the complete geometric parameters of 624 points (= single time steps) of the 500 K trajectories: 1) 208 points were arbitrarily chosen from normal periods, 2) the 208 observed crossover points of O−H···N → O···H−N transitions were included, and 3) 208 points were chosen from "ionic regions", where both hydrogen atoms are clearly trapped at the two nitrogen atoms. Similar to previous studies,[3] the crossover points were defined in terms of a proton-transfer reaction coordinate, $\rho = [R(OH)\cos\theta(HON)]/R(ON)$. A value of $\rho = 0.511$ was chosen, which is the appropriate value for the single proton-transfer transition state **1-3** obtained at the B3P86/6-31G++(d,p) level of theory (Table 1).

For convenience, in the subsequent discussion we distinguish between the two hydrogen bonds according to the nomenclature used for **1**, **1-3**, and **3** in Figure 1: $R(XY)′$ refers to bond lengths of initial O−H···N type groups, whereas $R(XY)″$ refers to bond lengths of initial O···H−N type

Table 1. Selected geometry,[a] and energy[b] and spectroscopy[c] data: A: average values from PAW trajectories for normal periods, crossover points, and ionic regions; B: theoretical data for **1**, **1-3**, and **3**.

	A		B		
	PAW normal periods	RHF	MP2 **1**	B3LYP	B3P86
(O−H)′	108 ± 7	97.7	102.8	104.7	106.7
(O···N)′	161 ± 16	181.0	163.4	157.8	150.5
(O···H)″	205 ± 32	206.9	193.5	188.8	180.9
(H−N)″	104 ± 4	100.0	101.9	102.5	103.0
(C−O)′	132 ± 3	129.8	132.1	131.1	130.0
(C=O)″	123 ± 3	119.7	123.4	122.7	122.8
(C=N)′	130 ± 3	127.0	129.7	129.5	129.3
(C−N)″	136 ± 4	134.0	135.2	134.4	133.6
(O···N)′	267 ± 12	278.6	266.1	262.4	257.1
(O···N)″	302 ± 27	303.8	293.2	289.0	282.0
C···C	400 ± 16	408.2	398.6	394.9	388.3
(O−H···N)′	166 ± 8	178	176	177	177
(O···H−N)″	156 ± 13	163	165	165	167
$\rho′$	0.401 ± 0.036	0.351	0.393	0.399	0.415
$\rho″$	0.668 ± 0.044	0.678	0.657	0.651	0.639
$\nu(OH′)$	2420	3766	3511	3373	3296
$\nu(NH″)$	3300	3483	2699	2384	2127
	crossover points		**1−3**		
(O···H)′	131 ± 3	127.8	131.0	128.6	127.1
(H···N)′	124 ± 3	119.3	118.7	121.6	121.9
(O···H)″	168 ± 15	180.9	167.6	167.1	162.6
(H−N)″	108 ± 4	101.6	104.6	105.3	105.8
(C−O)′	129 ± 3	126.0	128.7	128.1	127.1
(C=O)″	126 ± 3	122.2	125.8	124.9	124.6
(C=N)′	132 ± 3	128.5	130.8	130.6	130.3
(C−N)″	134 ± 4	131.5	132.7	132.7	132.2
(O···N)′	255 ± 7	247.1	249.7	250.2	248.9
(O···N)″	273 ± 12	280.3	271.3	271.4	267.6
C···C	381 ± 9	380.2	380.2	379.8	377.1
(O···H···N)′	169 ± 6	178	178	179	179
(O···H−N)″	162 ± 9	165	171	170	171
$\rho′$	0.511	0.514	0.525	0.514	0.511
$\rho″$	0.612 ± 0.029	0.643	0.617	0.614	0.606
	ionic regions		**3**		
O···H	156 ± 11	161.8	151.9	150.7	147.1
H···N	112 ± 6	104.5	108.3	109.5	110.2
C:O	127 ± 3	124.0	127.2	126.5	126.1
C:N	133 ± 4	129.8	131.6	131.5	131.2
O···N	265 ± 7	266.0	260.1	260.0	257.2
C···C	382 ± 9	382.4	379.7	379.1	376.1
O···H···N	166 ± 8	174	177	176	177
ρ	0.583 ± 0.028	0.608	0.584	0.579	0.572
$\nu(NH)_s$	(2200)	2996	2510	2386	2317
$\nu(NH)_a$		2854	2293	2182	2114
E(**1-3**)−E(**1**)		32.6	11.6	6.8	3.4
E(**3**)−E(**1**)		26.6	11.1	5.5	2.5

[a] Bond lengths in pm, angles in °. [b] Energy differences in kJ mol⁻¹. [c] Vibrational frequencies in cm⁻¹.

groups. The $R(ON)′$ distances of the points included in the sample data set are plotted against the corresponding $R(OH)′$ distances in Figure 4. At first glance the points are largely scattered, which gives some impression of the various geometries that are observed within the dynamic runs at temperatures of 500 to 600 K. Characteristic differences between the three classes of points (normal regions, crossover points, and ionic regions) can, nevertheless, be evaluated by considering average values as given in Table 1. In the case of $R(OH)′$ distances, despite significant scattering, the characteristic
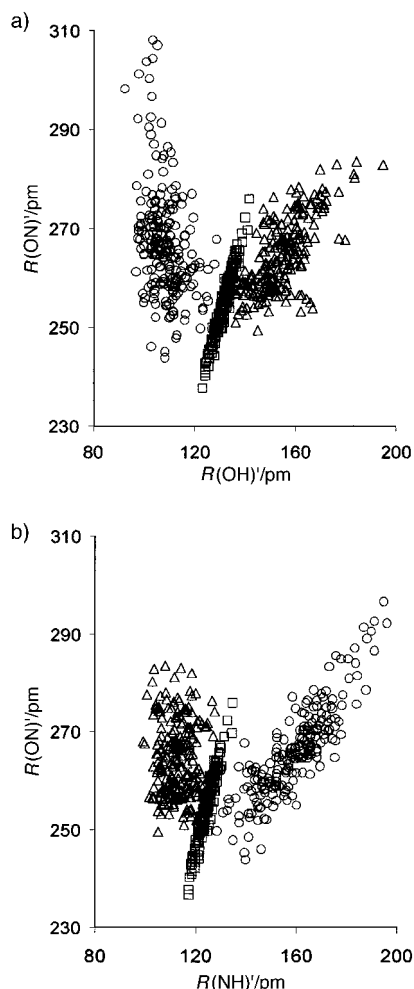
a)

b)

Figure 4. $R(\text{ON})$ versus a) $R(\text{OH})$ and b) $R(\text{NH})$ distances of normal periods (○), crossover points (□), and zwitterionic regions (△) (for the selection of points, see text).

differences are directly apparent from Figure 4, which is of course trivial, because the three classes are inherently defined by small, medium, and large $R(\text{OH})'$ distances. The average $R(\text{OH})'$ distances obtained from the data set are 108, 131, and 156 pm for normal regions, crossover points, and ionic regions, respectively. For the $R(\text{ON})'$ distances, the situation is not so evident from the purely visual view in Figure 4. However, on average we find similar $R(\text{ON})'$ distances for the normal and the ionic regions (267 and 265 pm, respectively), but significantly shorter $R(\text{ON})'$ distances for the crossover points (255 pm). In the case of normal regions and crossover points, the findings comply well with previous results[2, 3] of corresponding $R(\text{OO})$ distances in MA (264 and 238 pm), FAD (272 and 248 pm), and DHN (263 and 239 pm), although the differences are less pronounced for the present title compound. Hence, with all the examples studied so far, short $R(\text{X} \cdots \text{Y})$ distances were found to be a common characteristic of crossover points, and are therefore favorable for proton transfer to occur. It should, however, be emphasized that a shortening of the $R(\text{X} \cdots \text{Y})$ bond is not an essential "first step" in proton-transfer reactions, neither is proton transfer purely determined by $R(\text{X} \cdots \text{Y})$ distances, but by the full dynamics of the molecule or molecular complex. Previously, it

was shown by potential energy time evolutions[2, 3] that the proton motion may be understood reasonably well by considering the energy situation "experienced by the proton on the fly", which permanently changes owing to the full dynamics of the molecule.

Comparison with ab initio and DFT calculations: In Table 1, theoretical data are summarized for the gas-phase structures of **1**, **1-3**, and **3**, as obtained at various computational levels. The energy and geometry data comply well with those recently reported by Kim et al.[8] In particular, at all levels of theory: 1) The zwitterionic intermediate **3** was found to be a rather shallow, but true local minimum (confirmed by vibrational frequency calculations). 2) The single proton-transfer transition state **1-3** is an ordinary, first-order saddle point (also confirmed by vibrational frequency calculations). 3) Attempts to locate a stationary point that corresponds to the double proton-transfer transition state **1-2**, however, failed throughout.

It was noted in the introduction that based on their results, Kim et al.,[8] claimed that double proton transfer occurs asynchronously: **1** → **1-3** → **3** followed by **3** → **3-2** → **2**. In principle, this is just what we observe within the PAW trajectories. As discussed above, beginning at a normal situation with the two protons clearly trapped at an oxygen atom and at a nitrogen atom, double proton transfer always starts with proton transfer at the initial O−H′ ⋯ N group, and is followed by another proton transfer at the initial N−H″ ⋯ O group. In the majority of instances (83% successive processes), a zwitterionic intermediate is formed, which exists for a time period longer than an average ν(NH) vibrational cycle, whereas in the minority of instances (17% simultaneous processes), the second proton transfer follows too rapidly for the intermediate to be definitely formed for a reasonable time period.

At simulation temperatures of 500 – 600 K we are essentially not dealing with well-defined zero-temperature structures, but with vibrationally highly excited and hence largely distorted molecules. It can be seen in Figure 4 that the actual geometries of the individual time steps of a given class may vary significantly. Nevertheless, there should or even must be a close equivalence between the molecular geometries observed within the molecular dynamics runs and the optimized geometries of the prototropic species in Figure 1. Reasonably, in terms of Figure 1, the normal periods should correspond to the ground-state structure **1** (or to the symmetrically equivalent structure **2**). Furthermore, the ionic regions that result from O−H ⋯ N → O ⋯ H−N proton transfer should correspond to the zwitterionic intermediate **3**, and the crossover points should correspond to the transition state **1-3** (or to the symmetrically equivalent structure **2-3**).

Indeed, the expected correspondence between the stationary points **1**, **1-3**, and **3** on the one hand and the normal regions, the crossover points, and the ionic regions on the other hand, becomes clearly evident by considering average PAW geometries (Table 1). This is shown in Figure 5 for some selected bond lengths, for which theoretical data obtained at MP2/6-31G++(d,p) and B3P86/6-31G++(d,p) levels of theory are plotted along with the corresponding average PAW data
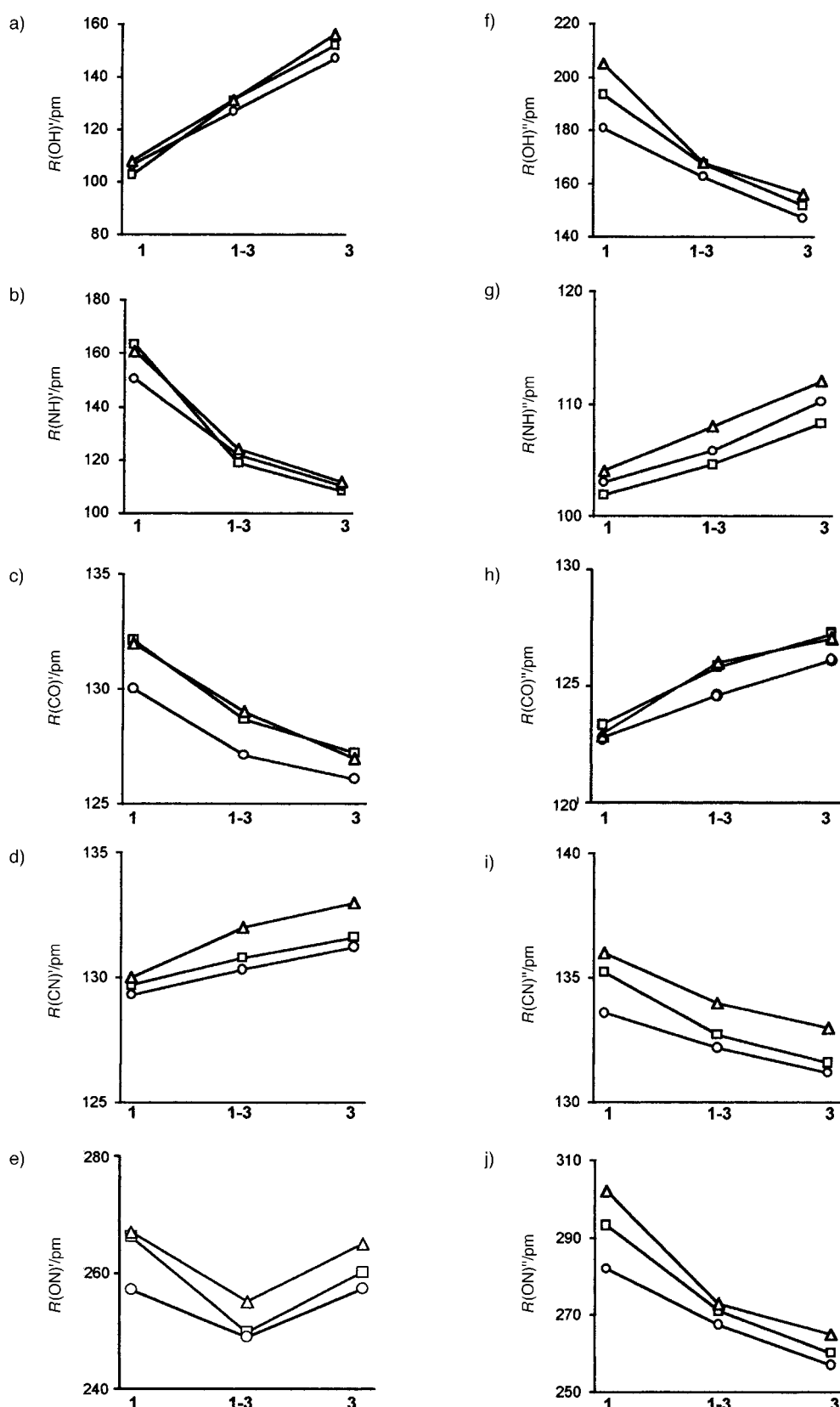
Figure 5. Comparison between selected bond lengths of **1**, **1-3**, and **3**, as obtained at MP2/6-31G++(d,p) (□) and B3P86/6-31G++(d,p) (○) levels of theory, and corresponding average PAW bond lengths (△) of normal periods, crossover points, and ionic regions.

as obtained from our sample data set (see also Table 1). The agreement between the theoretical and the (average) PAW bond lengths is certainly excellent, not only from a qualitative, but also from a quantitative point of view.

Double proton transfer in FFA, FAD, and DHN: To conclude, we briefly compare the preferred double proton-transfer mechanisms in the title compound with those in the two previously studied compounds DHN and FAD.[3] In the case of DHN, it was found that double proton transfer preferably takes place by means of a successive two-step mechanism with a delay between the two consecutive proton transitions of up to approximately 250 fs. On the contrary, it was found in the case of FAD that double proton transfer almost exclusively takes place by means of an almost simultaneous mechanism, with a delay between the two proton transitions of less than 12 fs. These differences were fully consistent with zero-temperature geometry optimizations. In the case of DHN, single proton transfer yields a metastable intermediate, namely the 4,8-dihydroxy-1,5-naphthoquinone tautomer, whereas in the case of FAD, single proton transfer does not result in a metastable intermediate. On the other hand, a double proton transition state could be located for FAD, but not for DHN.

In the case of FFA, the situation is similar to that of DHN. Single proton transfer at the initial O−H···N group yields a metastable intermediate, the zwitterionic structure **3**, whereas a double proton-transfer transition state **1-3** could not be located. Consequently, similar to the case of DHN, double proton transfer in FFA preferably (>80%) takes place by means of a successive two-step process, with a delay up to approximately 120 fs between the two proton transitions.

Conclusion

The finite-temperature PAW molecular dynamics study on proton motion and proton transfer in FFA reported herein integrates well with previous work on MA, DHN, and FAD.[2, 3] All proton-transfer processes start with a proton transition at the O−H···N group, which is followed by a second proton transition that involves either the same proton (single processes) or the other (N−H···O proton, double processes). Additionally, one may distinguish between simultaneous (or concerted) and successive processes. A limiting delay of 15 fs between the crossover points of the two transitions was chosen to ensure that in the latter cases, the zwitterionic intermediate that results from a proton transfer at the O−H···N group exists for a time period of at least one average ν(NH) vibrational cycle. According to this classification, the PAW trajectories revealed 42% concerted single crossing−recrossing transitions (including shuttling periods with several consecutive transitions), 16% successive single crossing−recrossing transitions (with a maximum delay of 115 fs), 7% simultaneous double proton transfers (with a minimum delay of 7 fs), and 35% successive double proton transfers (with a maximum delay of 120 fs).

The findings obtained from the PAW simulations are largely consistent with the results of ab initio and DFT calculations.

At all levels of theory, the zwitterionic intermediate that results from a single proton transfer at the O−H···N group is a true local minimum, whereas a transition state that corresponds to a true concerted double proton transfer could not be located. Hence from theoretical data, double proton transfer is expected to take place via the metastable zwitterionic intermediate. Furthermore, it was found that the optimized geometries of the stationary points (ground state, single proton-transfer transition state, zwitterion) comply excellently with the corresponding average geometry data of the normal periods, the crossover points, and the ionic regions obtained from the PAW trajectories.

Acknowledgements

[1] P. E. Blöchl, *Phys. Rev. B* **1994**, *50*, 17953.

[2] a) K. Wolf, W. Mikenda, E. Nusterer, K. Schwarz, *J. Mol. Struct.* **1998**, *448*, 201; b) K. Wolf, W. Mikenda, E. Nusterer, K. Schwarz, C. Ulbricht, *Chem. Eur. J.* **1998**, *4*, 1418.

[3] K. Wolf, A. Simperler, W. Mikenda, *Monatsh. Chem* **1999**, *130*, 1031.

[4] R. Car, M. Parrinello, *Phys. Rev. Lett.* **1985**, *55*, 2471.

[5] D. Marx, *Nachr. Chem. Tech. Lab.* **1999**, *47*, 186, and references therein.

[6] a) J. G. LePage, M. Alouani, D. L. Dorsey, W. John, *Phys. Rev. B* **1998**, *58*, 1499; b) T. Nukada, A. Bérces, M. Z. Zgierski, D. M. Whitfield, *J. Am. Chem. Soc.* **1998**, *120*, 13291; c) K. Schwarz, E. Nusterer, P. E. Blöchl, *Catal. Today* **1999**, *50*, 501; d) F. Terstegen, E. A. Carter, V. Buss, *Int. J. Quantum Chem.* **1999**, *75*, 141; e) T. K. Woo, P. M. Margl, L. Deng, L. Cavallo, T. Ziegler, *Catal. Today* **1999**, *50*, 479; f) H. M. Senn, P. E. Blöchl, A. Togni, *J. Am. Chem. Soc.* **2000**, *122*, 4098; g) T. K. Woo, T. Ziegler, *J. Organomet. Chem.* **1999**, *591,* 204.

[7] a) A. M. Sapse, C. S. Russell, *Int. J. Quantum Chem.* **1984**, *26*, 91; b) A. M. Sapse, C. S. Russell, *J. Mol. Struct. (Theochem)* **1986**,*137*, 43; c) J. Krechl, S. Böhm, S. Smrckova, J. Kuthan, *Collect. Czech. Chem. C.* **1989**, *54*, 673; d) I. Agranat, N. V. Riggs, L. Radom, *J. Chem. Soc. Chem. Comm.* **1991**, 80; e) A. Melo, M. J. Ramos, *Chem. Phys. Lett.* **1995**, *245*, 498; f) M. P. Fülscher, E. L. Mehler, *Chem. Phys.* **1996**, *204*, 403; g) L. Shimoni, J. P. Glusker, C. W. Bock, *J. Phys. Chem.* **1996**, *100*, 2957; h) Y.-J. Zheng, R. L. Ornstein, *J. Am. Chem. Soc.* **1996**, *118*, 11237; i) D. Peeters, G. Leroy, C. Wilante, *J. Mol. Struct.* **1997**, *416*, 21; j) A. Melo, M. J. Ramos, *Int. J. Quantum Chem.* **1999**, *72*, 157; k) A. Melo, M. J. Ramos, W. B. Floriano, J. A. N. F. Gomes, J. F. R. Leão, A. L. Magalhães, B. Maigret, M. C. Nascimento, N. Reuter, *J. Mol. Struct. (Theochem)* **1999**, *463*, 81.

[8] Y. Kim, S. Lim, Y. Kim, *J. Phys. Chem.* **1999**, *103*, 6632.

[9] a) S. Nagakawa, H. Umeyama, *J. Am. Chem. Soc.* **1978**, *100*, 7716; b) G. Lancelot, R. Mayer, C. Helene, *J. Am. Chem. Soc.* **1979**, *101*, 1569; c) D. J. Barlow, J. M. Thornton, *J. Mol. Biol.* **1983**, *168*, 867; d) J. Singh, J. M. Thornton, M. Snarey, S. F. Campbell, *FEBS Lett.* **1987**, *224*, 161; e) J. Andres, V. Moliner, J. Krechl, E. Silla, *J. Chem. Soc. Perkin Trans. 2* **1995**, 1551.

[10] a) S. Nosé, *Mol. Phys.* **1984**, *52*, 255; b) W. G. Hoover, *Phys. Rev. A* **1985**, *31*, 1695.

[11] J. P. Perdew, A. Zunger, *Phys. Rev. B* **1981**, *23*, 5048.

[12] D. Ceperley, B. J. Alder, *Phys. Rev. Lett.* **1980**, *45*, 566.

[13] a) A. D. Becke, *J. Chem. Phys.* **1992**, *96*, 2155; b) J. P. Perdew, *Phys. Rev. B* **1986**, *33*, 8822.

[14] M. J. Frisch, G. W. Trucks, H. B. Schlegel, G. E. Scuseria, M. A. Robb, J. R. Cheeseman, V. G. Zakrzewski, J. A. Montgomery, R. E. Strat-

mann, J. S. Burant, S. Dapprich, J. M. Millam, A. D. Daniels, K. N. Kudin, M. C. Strain, O. Farkas, J. Tomasi, V. Barone, M. Cossi, R. Cammi, B. Menucci, C. Pomelli, C. Adamo, S. Clifford, J. Ochterski, G. A. Petersson, P. Y. Ayala, Q. Cui, K. Morokuma, D. K. Malick, A. D. Rabuck, K. Raghavachari, J. B. Foresman, J. Cioslowski, J. V. Ortiz, B. B. Stefanov, G. Liu, A. Liashenko, P. Piskorz, I. Komaromi, R. Gomperts, R. L. Martin, D. J. Fox, T. Keith, M. A. Al-Laham, C. Y. Peng, A. Nanayakkara, C. Gonzales, M. Challacombe, P. M. W. Gill, B. G. Johnson, W. Chen, M. W. Wong, J. L. Andres, M. Head-Gordon, E. S. Replogle, J. A. Pople, Gaussian 98, Rev. A1, Gaussian, Inc., Pittsburgh, PA, **1998**.

[15] Complete geometry data of several hundred consecutive time frames (format: XYZ input file for Xmol) are available from the authors upon request.